

AD-~~291795~~ 110

*P. H. H.*

ASD-TDR-62-865

*42*

49834

CORRELATION OF PLATE CREEP BUCKLING THEORY  
WITH EXPERIMENTS ON LONG PLATES OF ALUMINUM  
ALLOY 2024-0 AT 500° F.

TECHNICAL DOCUMENTARY REPORT NO. ASD-TDR-62-865

**DISTRIBUTION STATEMENT A**

Approved for Public Release  
Distribution Unlimited

SEPTEMBER 1962

PROPERTY OF:

*PROPERTY OF THE AIR FORCE*

DIRECTORATE OF MATERIALS AND PROCESSES  
AERONAUTICAL SYSTEMS DIVISION  
AIR FORCE SYSTEMS COMMAND  
WRIGHT-PATTERSON AIR FORCE BASE, OHIO

PROJECT NO. 7351, TASK NO. 735106

(Prepared under Contract No. AF 33(657)-8233  
by New York University, New York, N.Y.;  
Ralph Papirno and George Gerard, authors.)

Reproduced From  
Best Available Copy

20020110 128

## NOTICES

When Government drawings, specifications, or other data are used for any purpose other than in connection with a definitely related Government procurement operation, the United States Government thereby incurs no responsibility nor any obligation whatsoever; and the fact that the Government may have formulated, furnished, or in any way supplied the said drawings, specifications, or other data, is not to be regarded by implication or otherwise as in any manner licensing the holder or any other person or corporation, or conveying any rights or permission to manufacture, use, or sell any patented invention that may in any way be related thereto.

Qualified requesters may obtain copies of this report from the Armed Services Technical Information Agency, (ASTIA), Arlington Hall Station, Arlington 12, Virginia.

This report has been released to the Office of Technical Services, U. S. Department of Commerce, Washington 25, D. C., for sale to the general public.

Copies of ASD Technical Reports and Technical Notes should not be returned to the Aeronautical Systems Division unless return is required by security considerations, contractual obligations, or notice on a specific document.

## FOREWORD

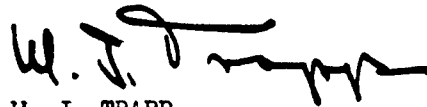
This report was prepared by New York University, New York, N. Y., under Contract No. AF 33(657)-8233. This contract was initiated under Project No. 7351, "Metallic Materials", Task No. 735106, "Behavior of Metals". The work was administered under the direction of the Directorate of Materials and Processes, Deputy for Technology, Aeronautical Systems Division, Wright-Patterson Air Force Base, Ohio, with Mr. D. M. Forney, Jr. acting as project engineer.

This report covers work conducted from February 1962 to August 1962.

# ABSTRACT

The results of creep-buckling experiments on long, simply-supported plates of aluminum alloy 2024-0 at 500°F under axial compression were correlated with a previously developed theory for perfect plates. Compressive-creep properties of the test material were obtained to develop the theoretical results. The plate experiments were performed using a square-tube configuration after an evaluation program indicated that the conventional vee groove-knife edge arrangement for simulating simple support was unsatisfactory for use at elevated temperatures. The theory was found to have predictive value for plate creep buckling when used in normalized form. A simplified approach for predicting creep crippling was also correlated with the test data. *Edg 11*

This technical documentary report has been reviewed and is approved.



W. J. TRAPP  
Chief, Strength and Dynamics Branch  
Metals and Ceramics Laboratory  
Directorate of Materials and Processes

## TABLE OF CONTENTS

	Page
1. INTRODUCTION . . . . .	1
2. SQUARE TUBE EXPERIMENTS . . . . .	3
3. TEST RESULTS . . . . .	5
4. CORRELATION OF TEST DATA WITH THEORY . . . . .	7
5. CONCLUSIONS . . . . .	11
6. REFERENCES . . . . .	12
APPENDIX . . . . .	25

# LIST OF ILLUSTRATIONS

Figure		Page
1	Square Tube Plate Specimen Installed in Instrumentation-Loading Jig . . . . .	13
2	Untested and Crippled Square Tube Plate Specimens . . . . .	13
3	Average Short Time Compression Stress Strain Curve of Aluminum Alloy 2024-0 at 500°F . . . . .	14
4	Compression Creep Curves of Aluminum Alloy 2024-0 for Various Applied Stress Levels at 500°F . . . . .	15
5	End Shortening and Lateral Deflection Data as a Function of Stress Level for Short Time Buckling and Crippling Experiments on Simply Supported Long Plates of Aluminum Alloy 2024-0 at 500°F with $b/h = 23$ . . . . .	16
6	End Shortening and Lateral Deflection Data as a Function of Time for Creep Buckling and Creep Crippling Experiments on Simply Supported Long Plates of Aluminum Alloy 2024-0 at 500°F with $b/h = 23$ . Applied Stress 8400 psi . . . . .	17
7	End Shortening and Lateral Deflection Data as a Function of Time for Creep Buckling and Creep Crippling Experiments on Simply Supported Long Plates of Aluminum Alloy 2024-0 at 500°F with $b/h = 23$ . Applied Stress 7840 psi . . . . .	17
8	End Shortening and Lateral Deflection Data as a Function of Time for Creep Buckling and Creep Crippling Experiments on Simply Supported Long Plates of Aluminum Alloy 2024-0 at 500°F with $b/h = 23$ . Applied Stress 7280 psi . . . . .	18
9	End Shortening and Lateral Deflection Data as a Function of Time for Creep Buckling and Creep Crippling Experiments on Simply Supported Long Plates of Aluminum Alloy 2024-0 at 500°F with $b/h = 23$ . Applied Stress 6720 psi . . . . .	18
10	Strain-Strain Rate Data Derived from Figure 4 . . . . .	19

# LIST OF ILLUSTRATIONS

(Continued)

Figure		Page
11	Constant Strain Rate Stress-Strain Data Derived from Figure 10 . . . . .	20
12	Effective Modulus-Stress Data for Long Flat Plates Under Axial Compression as Derived from Figure 11 . . . . .	21
13	Conditions for Creep Buckling of Long Flat Plates Under Axial Compression Derived from Figure 12 . . . . .	21
14	Correlation of Creep Buckling Theory and Experiments for Long Flat Plates of Aluminum Alloy 2024-0 at 500°F Under Axial Compression with $b/h = 23$ . . . . .	22
15	Correlation of Creep Buckling Theory with Experi- mental Creep Buckling Times for Long Flat Plates of Aluminum Alloy 2024-0 at 500°F Under Axial Compression with $b/h = 23$ Expressed in Normalized Form . . . . .	23
16	Correlation of Creep Buckling Theory and Secant Modulus Approach with Experimental Creep Crippling Times for Long Flat Plates of Aluminum Alloy 2024-0 at 500°F Under Axial Compression with $b/h = 23$ Expressed in Normalized Form . . . . .	24
17	End Shortening Data for Aluminum Alloy 2024-T3 at Room Temperature. Simple Support Simulated by Vee Groove-Knife Edge Jig . . . . .	30
18	End Shortening Data for Aluminum Alloy 2024-0 Plates with $b/h = 40$ at 500°F Shown with Comparable Short Time Compressive Stress Strain Data. Simple Support Simulated by Vee Groove-Knife Edge Jig . . . . .	30
19	End Shortening and Lateral Deflection Data for Creep Buckling Experiments on Aluminum Alloy 2024-0 Plates with $b/h = 25$ at 500°F Shown with Comparable Compressive Creep Data at an Applied Stress, $\sigma_a = 6720$ psi. Simple Support Simulated by Vee Groove-Knife Edge Jig. . . . .	31

# LIST OF SYMBOLS

$E$	modulus of elasticity, psi
$E_t$	tangent modulus, psi
$E_s$	secant modulus, psi
$b$	plate width, in.
$h$	plate thickness, in.
$k$	plate buckling coefficient
$w$	lateral deflection, in.
$z$	coordinate, in.
$\epsilon$	strain, micro-in/in.
$\dot{\epsilon}$	strain rate, micro-in/in/min.
$\epsilon_{cr}$	critical strain, micro-in/in.
$\eta$	plasticity reduction factor
$\eta_{\dot{\epsilon}}$	plasticity reduction factor - constant strain rate properties
$\nu$	Poisson's ratio
$\nu_e$	Poisson's ratio, elastic value
$\sigma$	stress, psi
$\sigma_a$	applied stress, psi
$\sigma_{cr}$	critical stress, psi
$\sigma_{cy}$	compression yield stress, psi
$\bar{\sigma}_f$	crippling stress, psi
	Subscript
$o$	short time conditions



## 1. Introduction

A theory of creep buckling of perfect plates and shells had been developed as part of the creep buckling investigation (1). It was the objective of the experimental program reported herein to obtain creep buckling data on long plates for correlation with the previously developed theory. In addition, test data on creep crippling were obtained and correlated with a proposed method of analysis.

### A. Boundary Conditions:

The major problem in performing buckling experiments whose results are to be correlated with theory, is simulating the mathematical boundary conditions required by the theory. If the theory described in Ref.(1) is applied to long plates, the boundary conditions along the loaded edges are not of major significance, although a small correction to the buckling coefficient would be necessary to take into account the actual elastic restraint at the ends.

The experimenter has a choice for the unloaded plate edges of using either clamped or simply supported edges since theoretical values of the buckling coefficient exist for each condition. Simulating clamped boundary conditions on the unloaded edges of a specimen plate and loading such a configuration however, present formidable difficulties in the laboratory. Simulating simple support boundary conditions, while not in the category of a routine laboratory operation, presents fewer difficulties than simulating clamped edges.

### B. Vee Groove-Knife Edge Simple Support Simulation:

A commonly used configuration for simple support on the unloaded edges of long plates employs a support jig containing vee grooves. The unloaded specimen edges are bevelled to fit into the grooves of the jig. Such a jig must meet the appropriate boundary conditions of zero lateral deflection and zero moment. In addition it must not introduce significant in-plane forces into the plate and it must offer little restraint to longitudinal compression of the plate. The ideal support jig would simulate the mathematically imposed boundary conditions as well as the other criteria while allowing plate growth due to thermal expansion and Poisson effects as well as allowing in-plane edge displacements due to buckling.

A support jig was constructed with the vee groove-knife edge configuration. A series of evaluation experiments, whose results are described in detail in the Appendix of this report, indicated that although this arrangement was satisfactory for room temperature experiments on elastic plates,

significant frictional effects developed at the 500°F test temperature in both short time buckling and creep buckling experiments. These anomalous effects were detected by comparing autographically recorded and shortening data from the buckling experiments with the appropriate compressive short time stress-strain data and compressive creep data obtained from independent tests on material property specimens.

#### C. Square Tube Configurations:

It was clear that frictional effects had to be eliminated in the experiments if the correlation of test data with creep buckling theory was to be meaningful. An experimental configuration in which the mathematical boundary conditions can be simulated and in which frictional effects are absent is the square tube. As is well known, this configuration of four orthogonal flat plates does simulate simple support since after buckling but prior to failure, the four unsupported edges remain straight ( $w = 0$ ) and the corner angle remains a right angle ( $\partial^2 w / \partial z^2 = 0$ ). In the past difficulties in obtaining such tubular material in aircraft structural alloys or difficulties in fabricating this configuration from solid stock have discouraged its use in stability studies of flat plates. However, in view of the serious limitations of jigs in simulating the boundary conditions without introducing extraneous effects into the specimen, it appeared that any extra efforts which would be required to fabricate square tube specimens would be justified.

Although it was not possible to obtain extruded square tubes in the 2024 aluminum alloy, extruded channel sections in this alloy were available. These were welded together to form the desired configuration using strips of the same alloy as the filler material.

The experiments described herein were conducted with square tube specimens of two wall thicknesses. A set of long thin wall specimens was used for the plate experiments and a set of shorter thick walled specimens for obtaining compressive short time stress-strain and compressive creep properties of the test material.

## 2. Square Tube Experiments

### A. Plate Specimens:

Extruded aluminum alloy 2024-T3 channel was received with the following cross section dimensions: thickness 1/8 in.; base width 1 in.; leg height 5/8 in. In order to fabricate plates with a thickness ratio of approximately 25, the thickness was uniformly reduced to 0.040 in. by machining the inner surfaces of the channel. This procedure maintained the 1 in. base width. The leg height was reduced to 1/2 in. and the free edges were externally bevelled to receive the filler material. Pairs of prepared channel sections were welded together to form square tubes using strips of the same aluminum alloy 2024-T3 as filler material. Excess filler material was machined away and the square tube sections were cut into 4-1/8 in. lengths with the ends held parallel within  $\pm 0.0005$  in. The specimens were then annealed to the "O" condition by the following heat treatment: 775°F 2 hrs.; cool to 500°F at 40°F/hr; furnace cool.

### B. Material Property Specimens:

Welded square tube specimens with the full 1/8 in. wall thickness and 3 in. long were fabricated in the same fashion as the specimens. These were annealed simultaneously with the plate specimens, thus assuring that all specimen material would undergo exactly the same heat treatment.

### C. Buckling Experiments on Plates at 500°F:

Instrumentation which had previously been developed for lateral deflection and end shortening measurements on the vee groove-knife edge configuration was adapted for use with square tube specimens. A parallelogram linkage employed for lateral deflection measured the maximum buckle amplitude present on the two opposite unwelded plates of the four plate configuration irrespective of where it occurred.

The end shortening measurements were made over a 3-5/8 in. gage length with gage points located 1/4 in. from the specimen ends on two opposite sides of the configuration. The separate end shortening measurements were electrically averaged. A jig was constructed to support the instrumentation and the various deflections were transferred out of the heated area to differential capacitor instrumentation.

A photograph of the installed specimen and instrumentation is shown in Figure 1. Also shown in the photograph is a bearing block used to transmit the load from the movable ram of the testing machine to the specimen. A second bearing block for the stationary ram is integral with the instrumentation jig.

Procedures, loading equipment and autographic recording instrumentation were identical to that employed previously in creep buckling experiments on

columns and are described in detail in Ref.(2).

The following experiments were performed, each in duplicate at 500°F:

1. Short time buckling and crippling.
2. Creep buckling and creep crippling at the following applied stress levels: 8400 psi, 7840 psi, 7280 psi, and 6720 psi. (Three experiments were performed at 7840 psi).

Crippling times ranged from several minutes to several hours over the range of applied stresses. Crippling was evidenced by the simultaneous rapid increase of end shortening and lateral deflection which occurred, as will be subsequently shown, when the lateral deflection reached approximately 60% of the thickness.

A crippled specimen together with an untested specimen is shown in Figure 2. It is evident that a number of buckle wave forms are present with one such wave form of slightly greater amplitude than the others. A careful examination of all tested plate specimens revealed that the maximum amplitude wave form did not occur in the same area in each specimen. This was an indication of lack of bias in the test procedure to favor a particular failure location.

#### D. Compressive Properties Tests at 500°F:

Using procedures, loading apparatus and autographic recording instrumentation as previously described in Ref.(2), both short time and creep properties in compression were obtained using 1/8 in. thick wall, welded square tube specimens. Strain was measured over a 2 in. gage length in the following tests, each performed in duplicate:

1. Short time compressive stress strain.
2. Compressive creep at the following applied stress levels: 8400 psi, 7840 psi, 7280 psi, and 6720 psi.

Care was taken during the experiments to maintain a strain rate during loading of approximately 0.04 in/in/min, the value which had been used in the short time and creep plate buckling experiments.

The scatter of the strain values both for the short time tests and the creep tests was found to be quite small. A maximum variation of  $\pm 2\%$  was found in the short time tests while the maximum scatter for the creep tests was found to be as follows:

8400 psi applied stress  $\pm 4.5\%$   
7840 psi applied stress  $\pm 0.9\%$   
7280 psi applied stress  $\pm 3.2\%$   
6720 psi applied stress  $\pm 4.6\%$

### 3. Test Results

#### A. Properties of the Test Material at 500°F:

The average short time compression stress strain curve of the aluminum alloy 2024-0 test material at 500°F is shown in Figure 3. Average compression creep curves of the specimen material are shown in Figure 4.

The most probable value of the compression modulus of elasticity at 500°F under the strain rate conditions of the test as determined from the short time tests and from the recorded stress strain curve during loading prior to creep tests was  $8.0 \times 10^6$  psi.

#### B. End Shortening and Lateral Deflection Data from Buckling Tests at 500°F:

End shortening and lateral deflection data as a function of stress level from short time buckling tests are shown in Figure 5. Also shown in the figure is the average short time compression stress strain curve.

End shortening and lateral deflection data as a function of time are shown in Figures 6 through 9 for the following applied stress levels: 8400 psi, 7840 psi, 7280 psi and 6720 psi. In one experiment at 8400 psi there was instrumental failure in the end shortening recording system, hence the data are not given.

Also shown in the figures are the appropriate creep curves for comparison with the end shortening data. In computing the value of the plate width to thickness ratio it has been shown in Ref.(3) that the inside width of the square tube is the pertinent measurement to be used. The appropriate value for the width to thickness ratio for the specimens used in this investigation was then  $b/h = 23.0$ .

#### C. Discussion of Experimental Results:

The end shortening curve closely follows the pertinent stress-strain or creep curve in most experiments until significant lateral deflections occur. This is an indication that the instrumentation and its supporting jig introduce little restraint to the square tube plate specimens. It is interesting to note that the first appearance of lateral deflections appears to have little influence on the end shortening curve, hence the latter is an insensitive indication of plate buckling. Plate crippling however is accompanied by a large increase of end shortening.

Since it is difficult, experimentally, to fabricate and test a perfect plate specimen, the choice of where buckling first occurs in terms of lateral deflection becomes more or less arbitrary. In three experiments however, the specimens were sufficiently "perfect" such that lateral deflections occurred quite suddenly with a sharp break in the lateral deflection curve. These were the two short time experiments and one creep buckling experiment at

7280 psi (specimen No. 23).

D. Accuracy of the Data:

The loading equipment and recording instrumentation used in this study were the same as had been used previously for studies on columns. The statement on experimental accuracy given in Ref.(2) as applied to equipment and instrumentation would apply to the current experiments. Major sources of error are summarized below:

1. Extensometer stability  $\pm 0.1\%$  per day.
2. Maximum extensometer error  $\pm 1\%$ .
3. Maximum loading system error  $\pm 0.5\%$ .
4. Maximum spatial and temporal temperature variation  $\pm 2^\circ\text{F}$ .
5. Recorder stability  $\pm 0.25\%$  per month.
6. Timing errors were negligible.

#### 4. Correlation of Test Data with Theory

In the correlation of plate buckling data with theory an inherent difficulty lies in establishing from the experimental data when buckling has occurred. This is due to the fact that a plate in a short time test can continue to support increasing loads after buckling and sudden collapse does not occur until the crippling or failure load is reached. The latter can be considerably in excess of the buckling load. In the case of creep experiments where a constant load is applied the plate can continue to support the applied loading for relatively long times after buckling.

The use of a lateral deflection criterion for buckling of imperfect plates is far from ideal since the degree of imperfection will influence the lateral deflection values. However, in the absence of other more rational criteria, we have arbitrarily assumed that buckling has occurred when the lateral deflection reaches 5% of the plate thickness. In the few relatively "perfect" specimens the buckling stress was chosen to coincide with a sharp break in the lateral deflection curve.

##### A. Short Time Buckling:

An appropriate solution for the short time plastic buckling of long simply supported plates has been given in Ref.(4) as:

$$\sigma_{cr} = \frac{\pi^2 k \eta E}{12(1-\nu_e^2)} \left(\frac{h}{b}\right)^2 \quad (1)$$

where

$$\eta = \frac{(1-\nu_e^2)}{(1-\nu^2)} \frac{E_s}{2E} \left[ 1 + \left( \frac{1}{4} + \frac{3}{4} \frac{E_t}{E_s} \right)^{1/2} \right] \quad (2)$$

and

$$\nu = 0.5 - 0.2 E_s/E \quad (3)$$

For very long simply supported plates,  $k = 4$ . However, in the experiments performed the aspect ratio of the plates was approximately 4 and the loaded edges could be considered clamped. In this case it is shown in Ref. 4 that  $k = 4.15$ .

From Eq.(1)

$$\frac{\sigma_{cr}}{\eta E} = \frac{\pi^2 k}{12(1-\nu_e^2)} \left(\frac{h}{b}\right)^2 \quad (4)$$

Using the appropriate values in Eq.(4)

$$\frac{\sigma_{cr}}{\eta E} = 0.00709 \quad (5)$$

The left hand side of Eq.(5) can be evaluated with the aid of Eqs.(2) and (3) and the short time compression stress-strain curve to find the value of  $\sigma_{cr}$  which corresponds to Eq.(5). This value has been found to be  $\sigma_{cr} = 10.0$  ksi.

Referring to Figure 5, sharp breaks in the lateral deflection curves for the two specimens shown occur at 10.4 ksi and 10.2 ksi. With this criterion of buckling, the errors are +4% and +2% respectively. The source of this discrepancy has not been determined, however a similar discrepancy was observed in the short time buckling of aluminum alloy columns at 500°F as reported in Ref. 6. The probable cause of this discrepancy for the plates is believed to be the stiffening effect of small radii at the inner corners of this square tube.

#### B. Creep Buckling:

In Ref.(1) it was shown that creep buckling solutions are analogous to plastic buckling solutions as given by Eq.(1) with the stipulation that the value of  $\eta$  becomes  $\eta_{\dot{\epsilon}}$ . The subscript here indicates that the appropriate material properties are derived from constant strain rate stress-strain curves which in turn are derived by a graphical process from the compressive creep data. The process is described in detail in Ref.(1) but is summarized below:

The compressive creep curves given in Figure 4 are graphically differentiated to obtain strain-strain rate data as shown in Figure 10. Constant strain rate stress-strain curves from this data and shown in Figure 11 are analyzed to obtain  $\eta_{\dot{\epsilon}}$  and  $\nu$ . On a plot of  $\eta_{\dot{\epsilon}} E$  and  $\sigma$  a straight line corresponds to a particular value of the  $b/h$  ratio. Shown in Figure 12 are such data with the straight line appropriate to  $b/h = 23$  and  $k = 4.15$ , the conditions for our experiments. Each intersection of this straight line with the curves of  $\eta_{\dot{\epsilon}} E$  represents an unique set of conditions for creep buckling which have been given in Figure 13. In order to predict creep buckling times, one first finds the appropriate strain rate for buckling for the applied stress level from Figure 13. Then using an inverse process one uses Figure 10 and Figure 4 to determine the theoretical creep buckling times.

Using the process outlined above, the theoretical curve shown as the solid curve in Figure 14 was obtained. Shown in the figure by open circles are the experimental times for lateral deflections to reach 5% of the thickness which we have arbitrarily designated as the buckling time. The crippling or failure times have been indicated on Figure 14 by closed circles. The



data presented in the figure were obtained from Figures 6 through 9. Short time data from Figure 5 are also given in Figure 14. It is evident from the figure that the short time discrepancy is reflected in the creep buckling results. This result was previously observed for the column tests of Ref.(6).

An approach to creep crippling involves the use of the secant modulus as described in Ref.(7). If it is assumed that

$$\eta = E_s/E \quad (6)$$

and Eq.(6) is substituted in Eq.(4)

$$\frac{\sigma_{cr}}{E_s} = \frac{\pi^2 k}{12(1-\nu_e^2)} \left(\frac{h}{b}\right)^2 \quad (7)$$

But

$$E_s = \sigma/\epsilon \quad (8)$$

Hence

$$\epsilon_{cr} = \frac{\pi^2 k}{12(1-\nu_e^2)} \left(\frac{h}{b}\right)^2 \quad (9)$$

Using the appropriate values in the right hand side of Eq.(9) results in

$$\epsilon_{cr} = 7090 \text{ micro-in/in} \quad (10)$$

Eq.(10) implies that the plate will cripple when the end shortening strain reaches the value computed. The secant modulus results are shown as the broken curve in Figure 14.

#### C. Normalized Stress Representation of Creep Buckling:

A more rational correlation between the creep buckling data and the theory can be made if the discrepancy in the short time results are suppressed, in view of the apparent dependence of creep buckling upon the short time buckling behavior. This can be accomplished by normalizing the theoretical creep buckling stresses to the appropriate short time theoretical critical stresses and by normalizing the applied stresses to the appropriate short time buckling stresses for the experiments. Such a normalized representation is shown in Figure 15. The normalized data are in

substantial agreement with the normalized theory indicating the procedure to be valid for the prediction of creep buckling times.

#### D. Normalized Stress Representation of Creep Crippling:

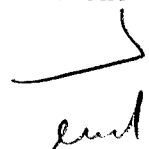
Although the constant strain rate theory was developed for the buckling of plates, it seemed interesting to examine its predictive value for plate crippling in normalized form. The theoretical creep buckling curve was normalized as before. The experimental applied stresses were normalized to the short time crippling stresses. The results of this normalizing procedure are given in Figure 16 as the solid curve. A similar normalizing procedure was applied to the secant modulus hypothetical approach and the results are shown in Figure 16 as the broken curve. As in the case of creep buckling the data are in substantial agreement with both the constant strain rate approach and the secant modulus approach. In view of the facility with which the secant modulus hypothesis can be applied, it could be recommended for prediction of creep crippling times when used in normalized form.

## 5. Conclusions

A rather significant conclusion that is apparent from the test data analyzed herein for aluminum alloy 2024-0 simply supported plates at 500°F as well as data previously analyzed for columns in Ref.(6) is concerned with the short time buckling stresses at elevated temperatures. It appears that the elevated temperature buckling stress can significantly exceed the corresponding theoretical value. The short time behavior is reflected in the creep buckling and creep crippling results. As a consequence of this short time behavior, it is necessary to correlate creep buckling theory with test data on a non-dimensional stress basis.

At the normalized representation the constant strain rate creep buckling theory represents a lower bound for creep buckling. The secant modulus approach shows reasonably good correlation with the creep crippling test data. It would appear that the constant strain rate theory is associated with the initial development of lateral deflections in the plates and the secant modulus is associated with crippling or failure of the plates. Thus it is concluded that the constant strain rate plate creep buckling theory has distinct predictive value for creep buckling.

The results and conclusions of this investigation suggest that short time elevated temperature tests of plates are required to establish a base point for creep buckling and creep crippling. Using this base point the normalized constant strain rate plate creep buckling theory may be utilized to construct absolute creep buckling predictions. The normalized secant modulus approach appears to provide a particularly simple approach for the prediction of creep crippling of plates.



## 6. References

1. Gerard, George, "Investigation of Creep Buckling of Columns and Plates Part V: Theory of Creep Buckling of Perfect Plates and Shells," Technical Documentary Report No. WADC TR 59-416 Part V, February 1962.
2. Papirno, Ralph and Gerard, George, "Investigation of Creep Buckling of Columns and Plates Part II: Creep Buckling Experiments with Columns of Ti-7Al-4Mo Titanium Alloy," WADC TR 59-416 Part II, July 1960.
3. Becker, Herbert, "Handbook of Structural Stability Part II - Buckling of Composite Elements," NACA Technical Note 3782, July 1957.
4. Gerard, George and Becker, Herbert, "Handbook of Structural Stability Part I - Buckling of Flat Plates," NACA Technical Note 3781, July 1957.
5. Gerard, George, "Handbook of Structural Stability Part IV - Failure of Plates and Composite Elements," NACA Technical Note 3784, August 1957.
6. Gerard, George and Papirno, Ralph, "Classical Columns and Creep," Journal of The Aerospace Sciences, Vol. 29, No. 6, pp. 680-688, June 1962.
7. Gerard, George, "A Creep Buckling Hypothesis," Journal of the Aeronautical Sciences, Vol. 23, No. 9, pp. 879-882, September 1956.

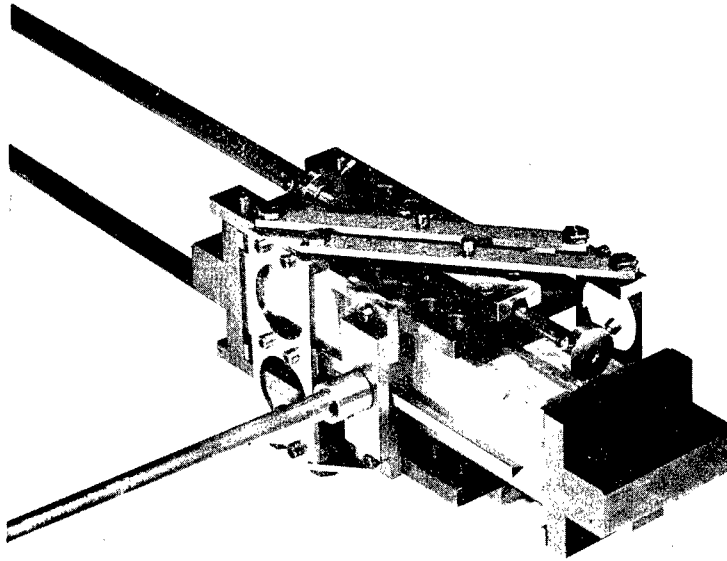


FIGURE 1 SQUARE TUBE PLATE SPECIMEN INSTALLED  
IN INSTRUMENTATION-LOADING JIG.

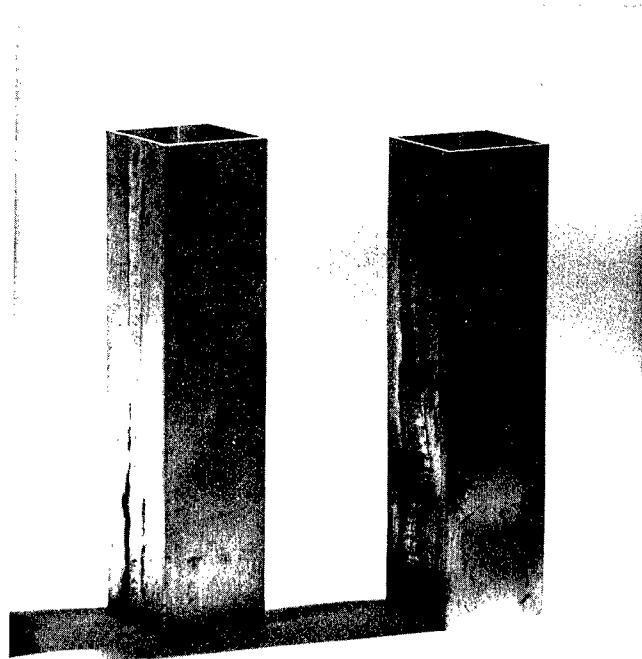


FIGURE 2 UNTESTED AND CRIPPLED SQUARE  
TUBE PLATE SPECIMENS.

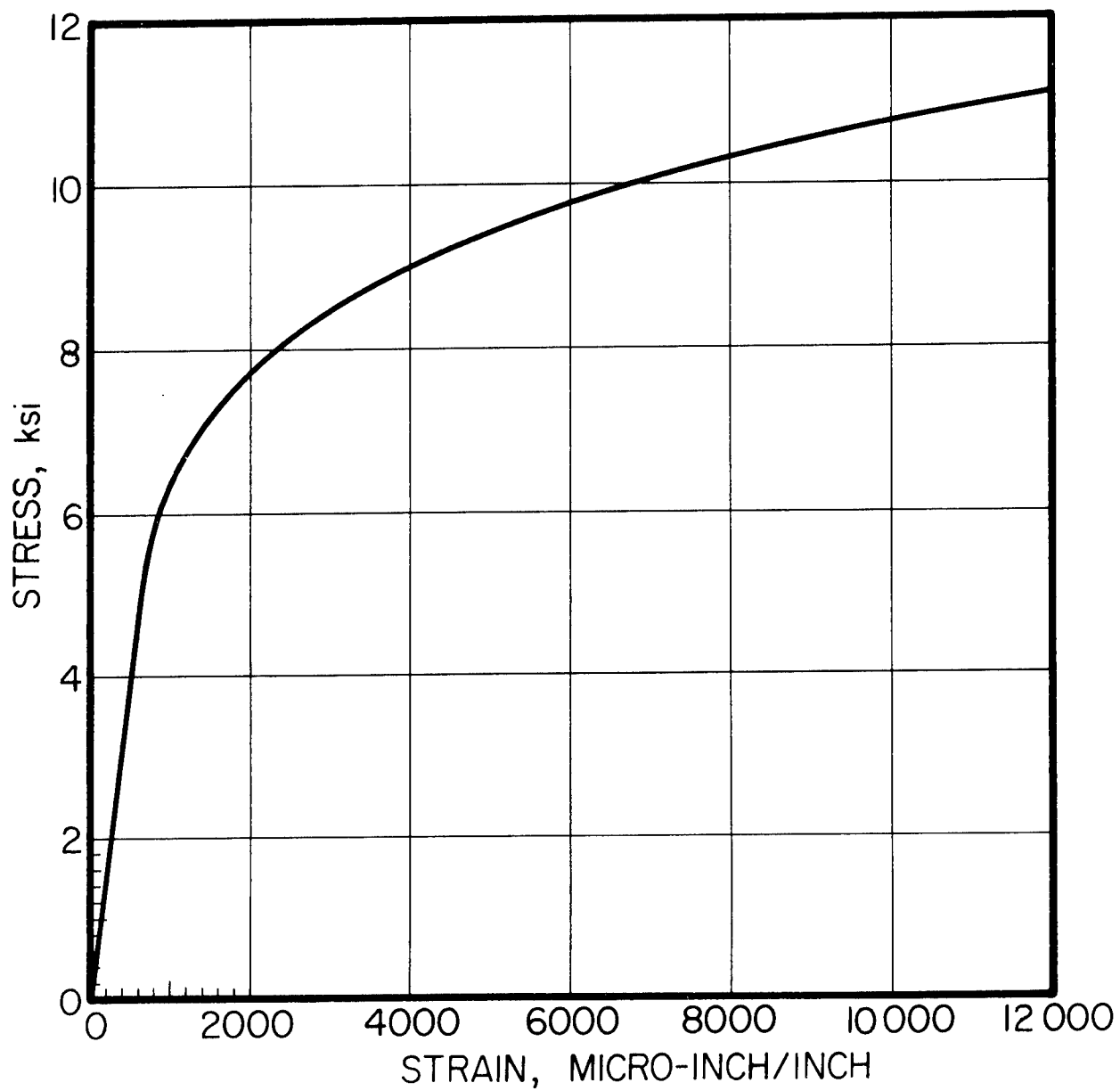


FIGURE 3 AVERAGE SHORT TIME COMPRESSION STRESS STRAIN  
CURVE OF ALUMINUM ALLOY 2024-0 AT 500°F.

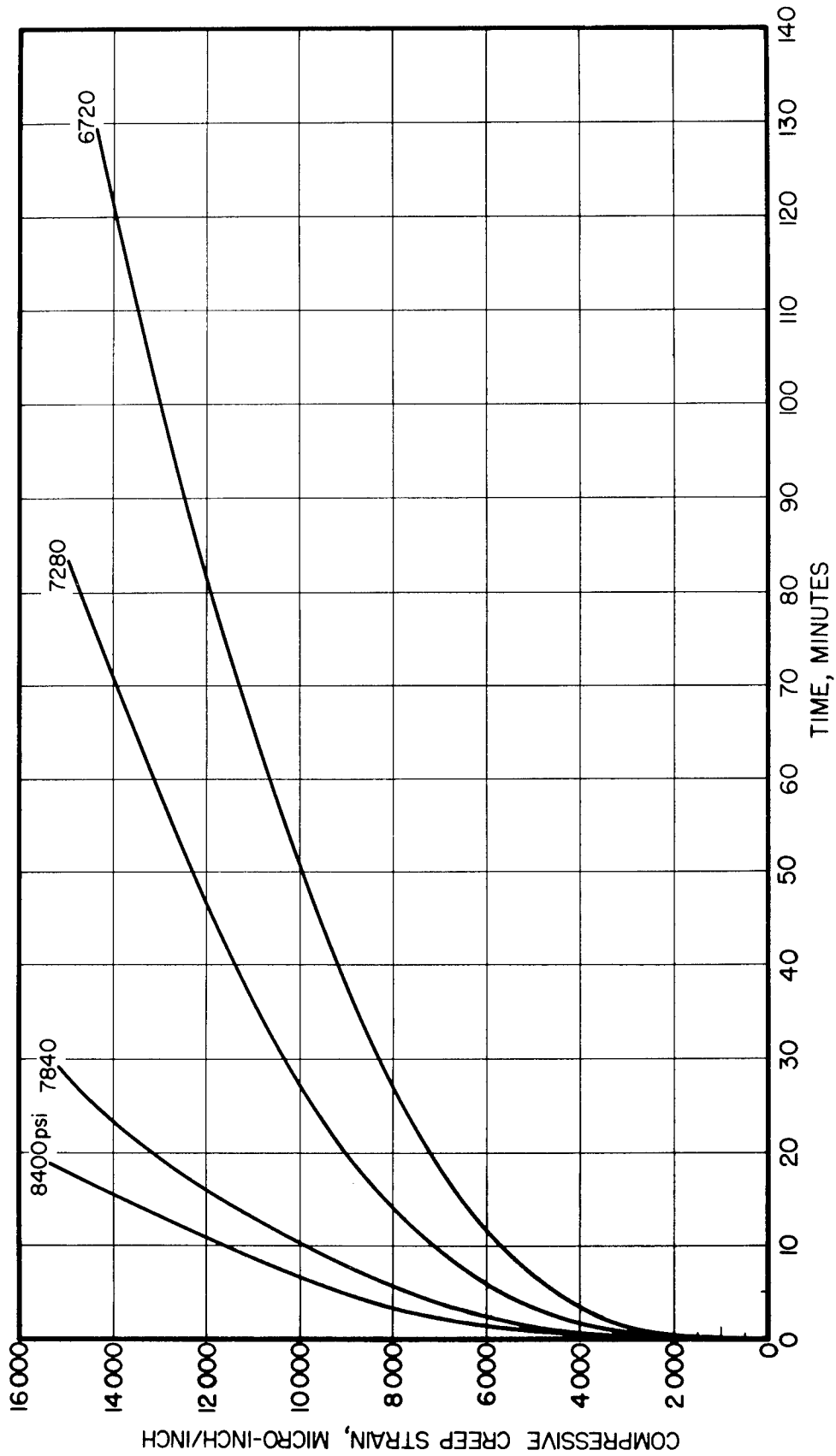


FIGURE 4 COMPRESSION CREEP CURVES OF ALUMINUM ALLOY 2024-0  
FOR VARIOUS APPLIED STRESS LEVELS AT 500°F.

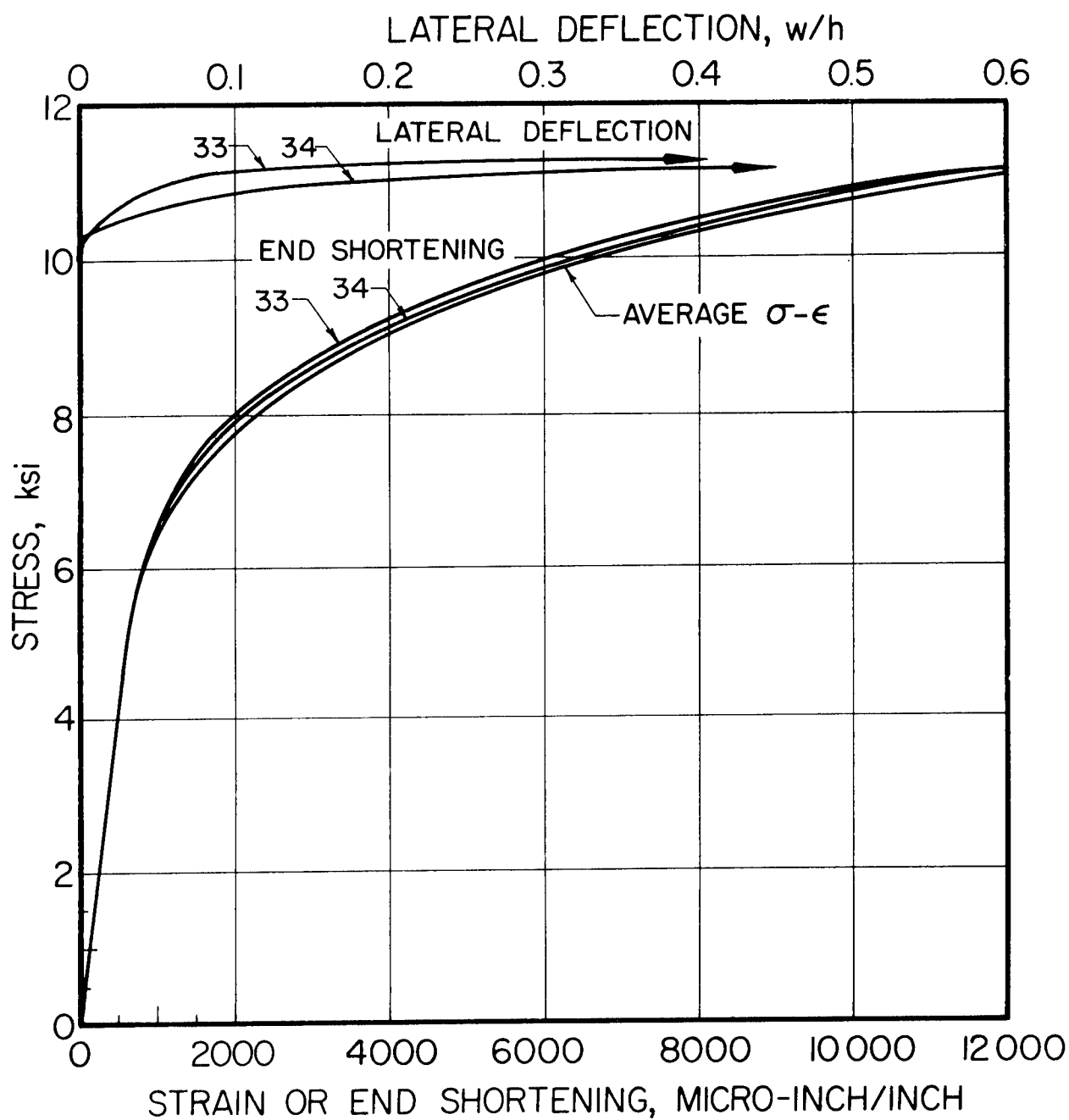


FIGURE 5 END SHORTENING AND LATERAL DEFLECTION DATA AS A FUNCTION OF STRESS LEVEL FOR SHORT TIME BUCKLING AND CRIPPLING EXPERIMENTS ON SIMPLY SUPPORTED LONG PLATES OF ALUMINUM ALLOY 2024-O AT 500°F WITH  $b/h = 23$ .



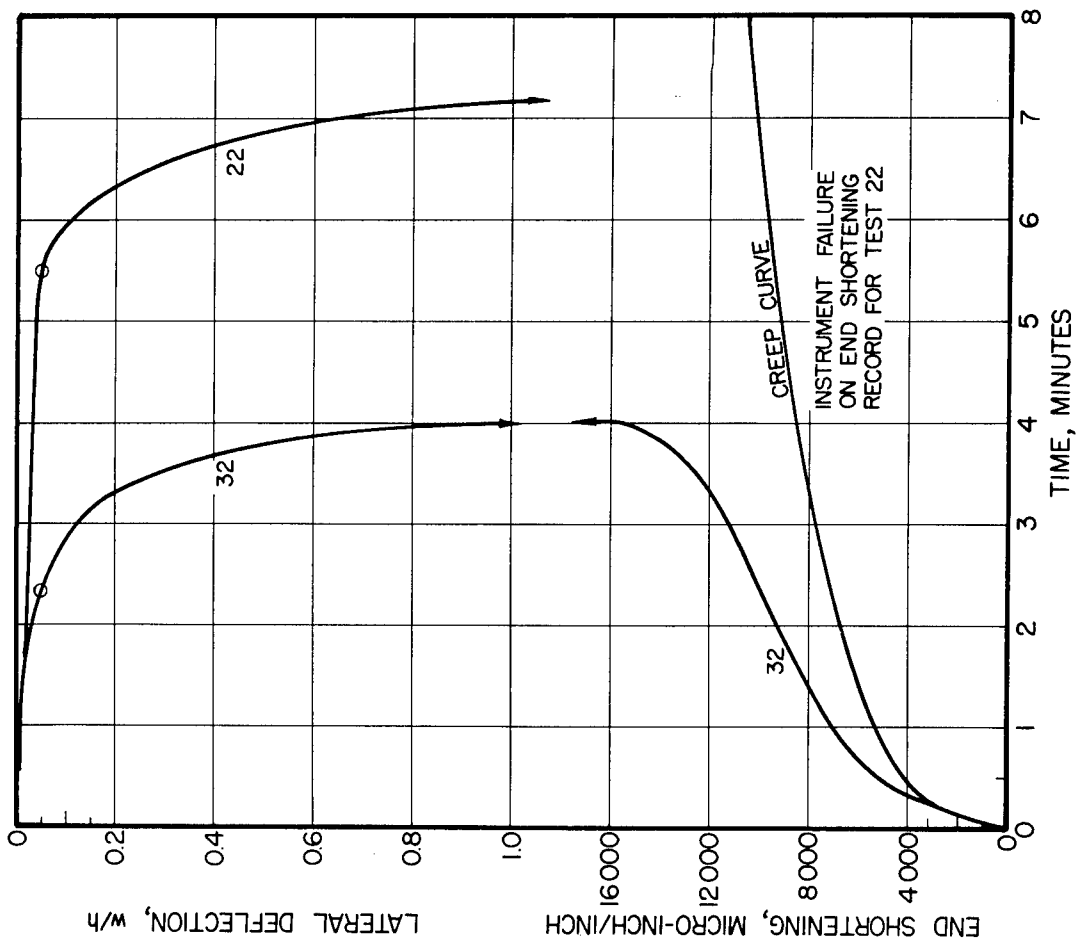


FIGURE 6 END SHORTENING AND LATERAL DEFLECTION DATA AS A FUNCTION OF TIME FOR CREEP BUCKLING AND CREEP CRIPPLING EXPERIMENTS ON SIMPLY SUPPORTED LONG PLATES OF ALUMINUM ALLOY 2024-0 AT 500°F WITH  $b/h = 23$ . APPLIED STRESS 8400 psi.

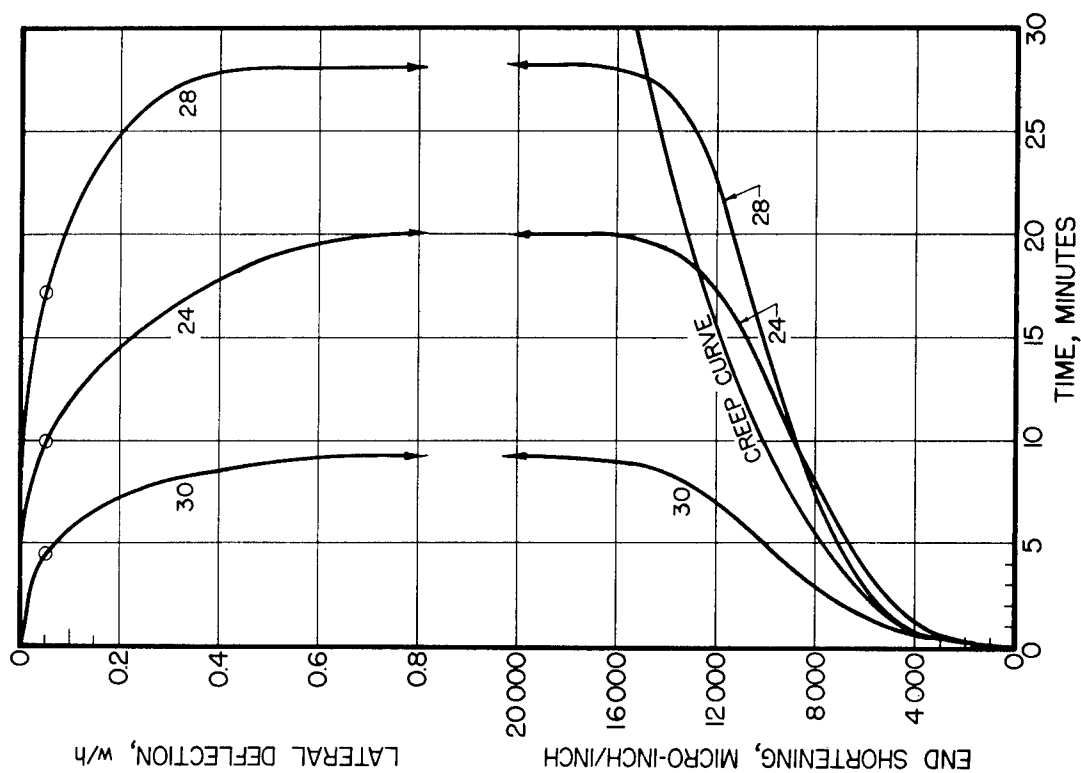


FIGURE 7 END SHORTENING AND LATERAL DEFLECTION DATA AS A FUNCTION OF TIME FOR CREEP BUCKLING AND CREEP CRIPPLING EXPERIMENTS ON SIMPLY SUPPORTED LONG PLATES OF ALUMINUM ALLOY 2024-0 AT 500°F WITH  $b/h = 23$ . APPLIED STRESS 7840 psi.

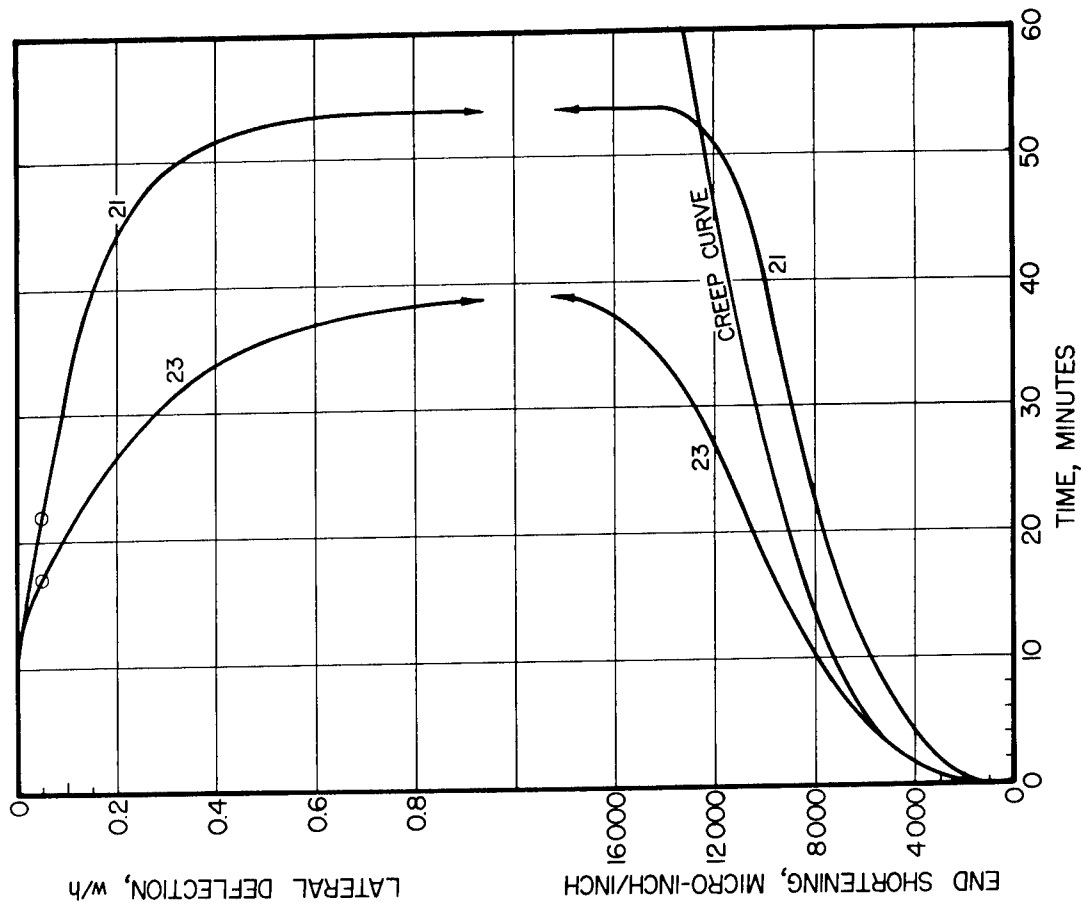


FIGURE 8 END SHORTENING AND LATERAL DEFLECTION DATA AS A FUNCTION OF TIME FOR CREEP BUCKLING AND CREEP CRIPPLING EXPERIMENTS ON SIMPLY SUPPORTED LONG PLATES OF ALUMINUM ALLOY 2024-T3 AT 500°F WITH  $b/h = 23$ . APPLIED STRESS 7280 psi.

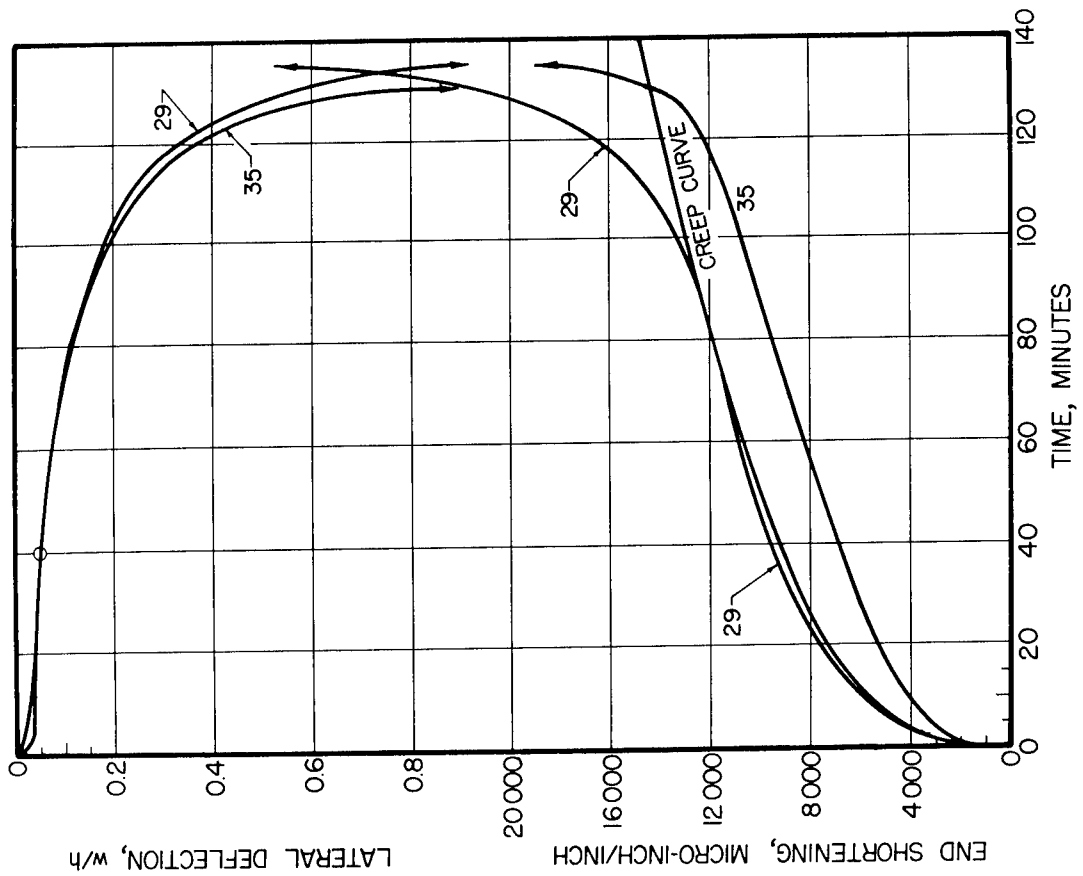


FIGURE 9 END SHORTENING AND LATERAL DEFLECTION DATA AS A FUNCTION OF TIME FOR CREEP BUCKLING AND CREEP CRIPPLING EXPERIMENTS ON SIMPLY SUPPORTED LONG PLATES OF ALUMINUM ALLOY 2024-T3 AT 500°F WITH  $b/h = 23$ . APPLIED STRESS 6720 psi.

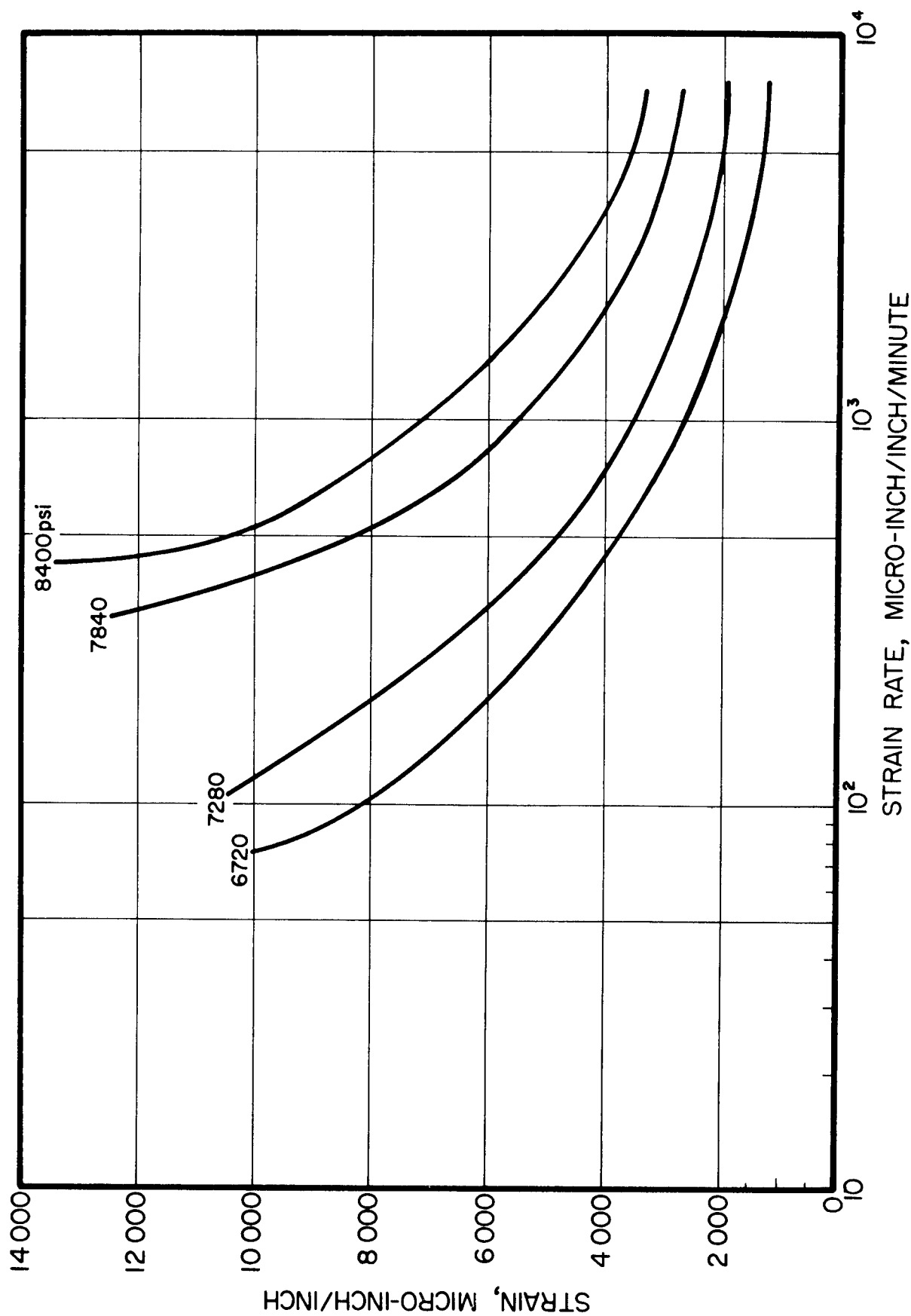


FIGURE 10 STRAIN-STRAIN RATE DATA DERIVED FROM FIGURE 4.

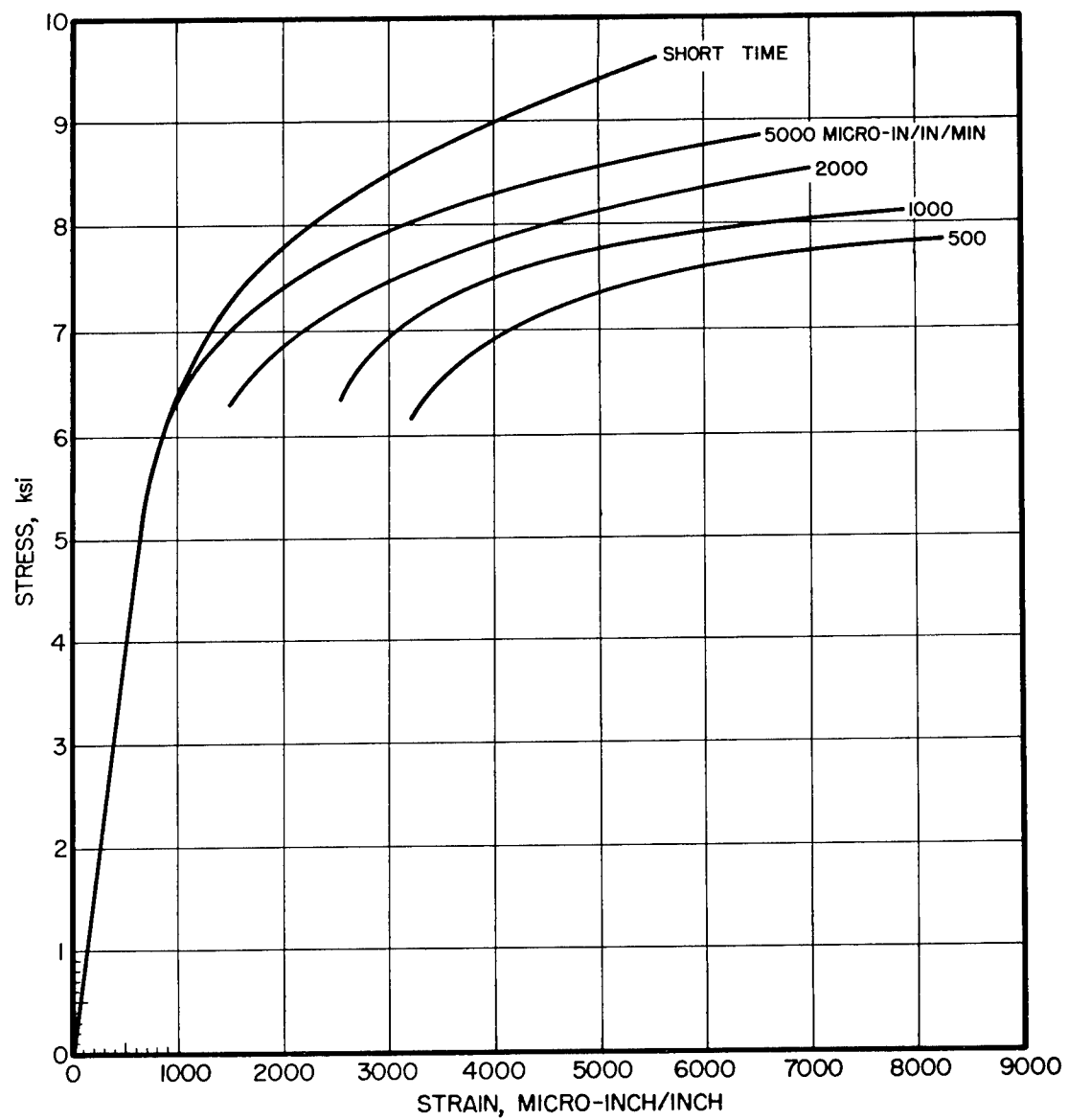


FIGURE 11 CONSTANT STRAIN RATE STRESS-STRAIN  
DATA DERIVED FROM FIGURE 10.

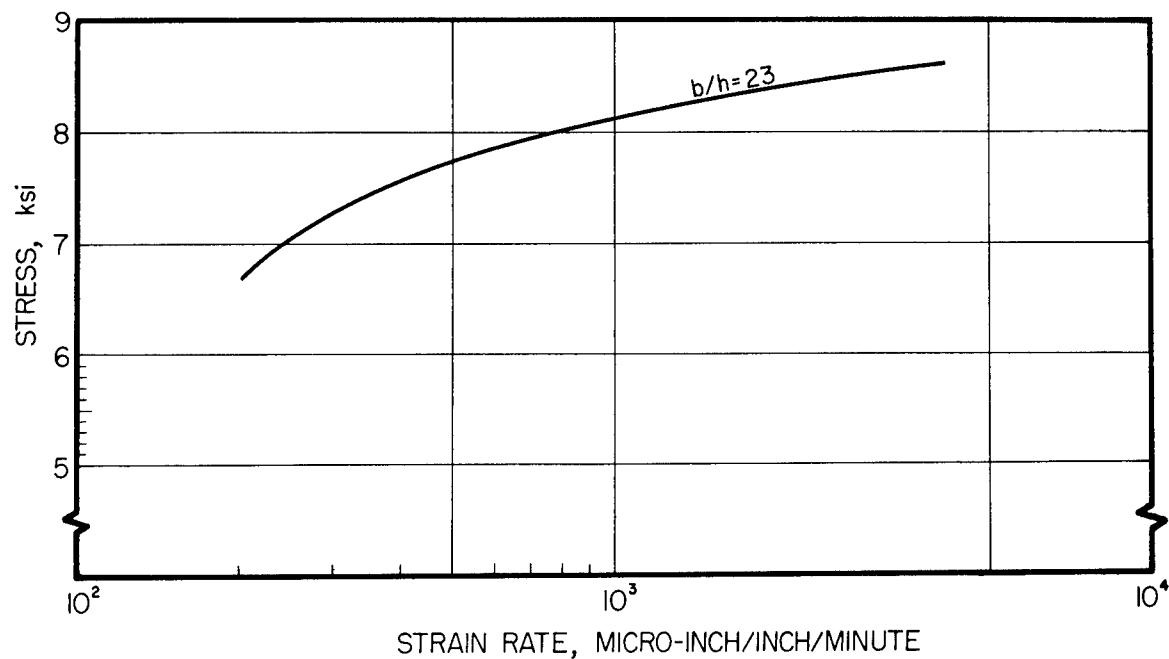


FIGURE 12 EFFECTIVE MODULUS-STRESS DATA FOR LONG FLAT PLATES UNDER AXIAL COMPRESSION AS DERIVED FROM FIGURE 11.

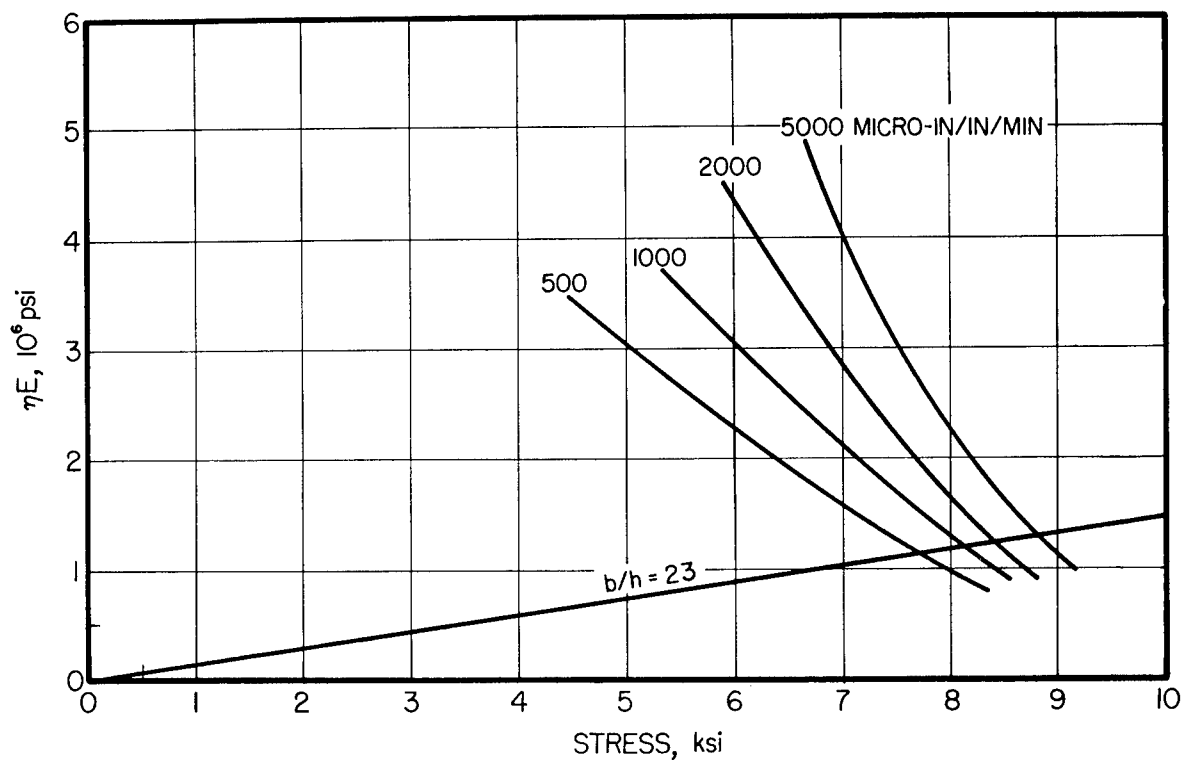


FIGURE 13 CONDITIONS FOR CREEP BUCKLING OF LONG FLAT PLATES UNDER AXIAL COMPRESSION DERIVED FROM FIGURE 12.

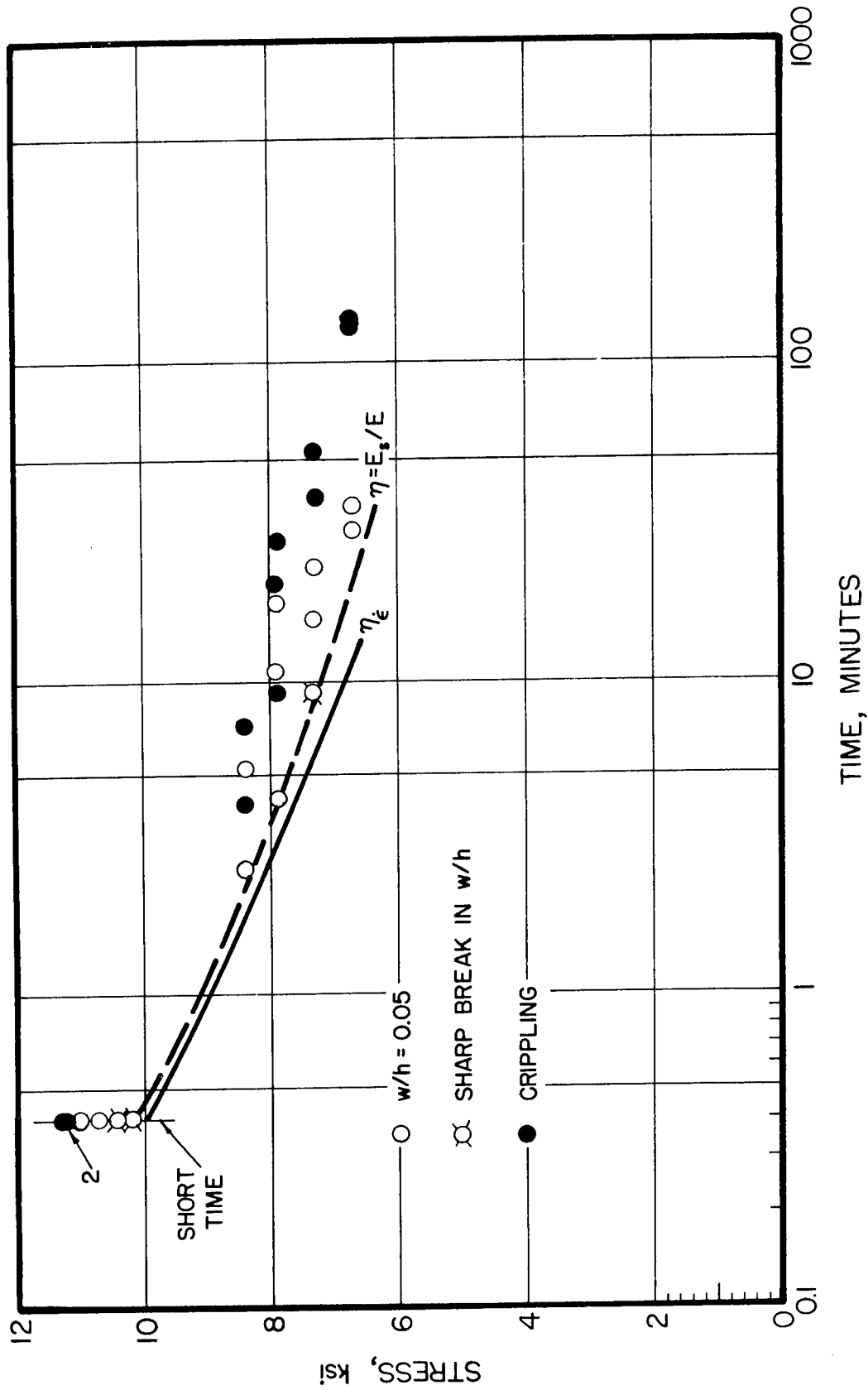


FIGURE 14 CORRELATION OF CREEP BUCKLING THEORY AND EXPERIMENTS FOR LONG FLAT PLATES OF ALUMINUM ALLOY 2024-T3 AT 500°F UNDER AXIAL COMPRESSION WITH  $b/h = 23$ .

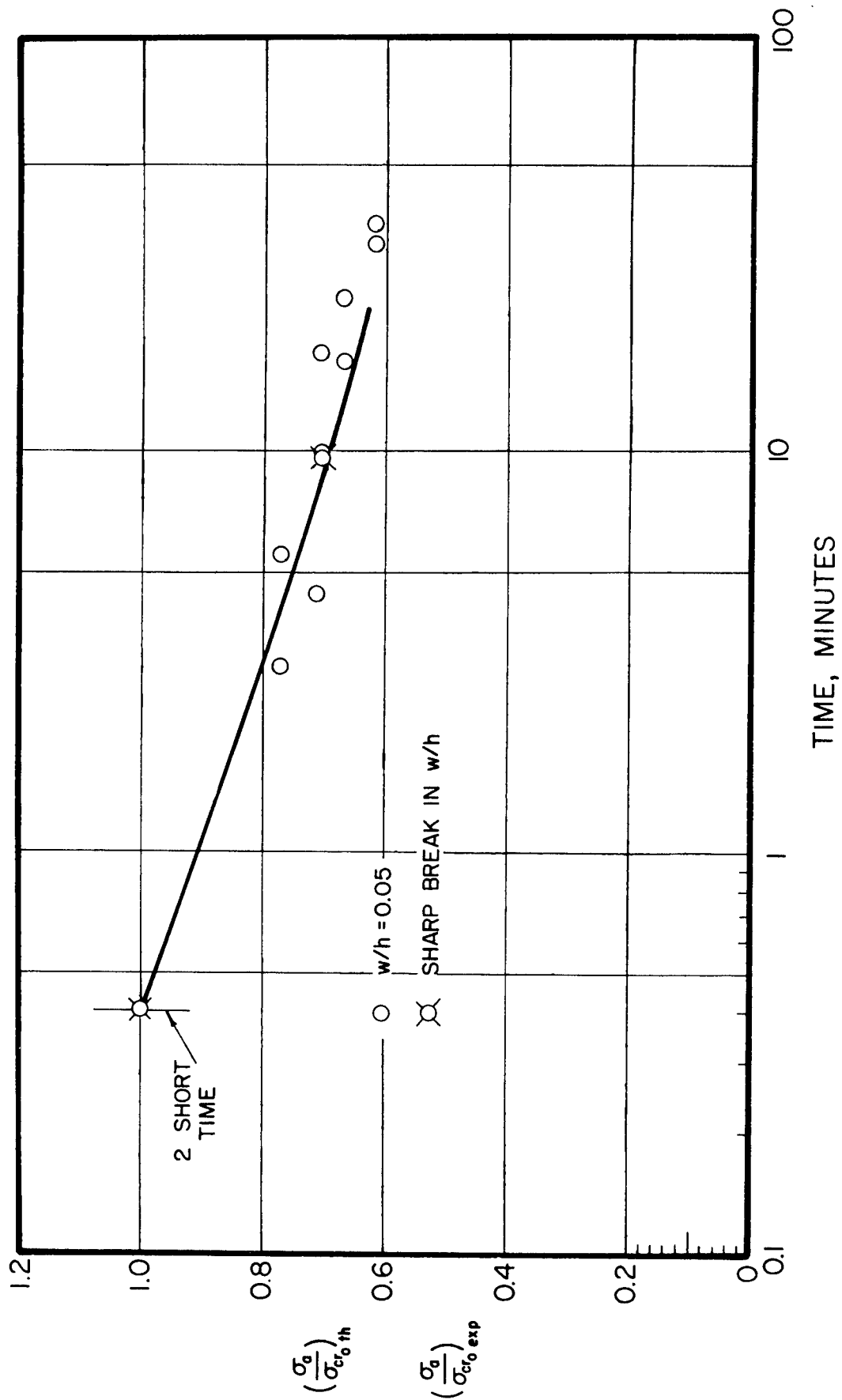


FIGURE 15 CORRELATION OF CREEP BUCKLING THEORY WITH EXPERIMENTAL CREEP BUCKLING TIMES FOR LONG FLAT PLATES OF ALUMINUM ALLOY 2024-T3 AT 500°F UNDER AXIAL COMPRESSION WITH  $b/h = 23$  EXPRESSED IN NORMALIZED FORM.

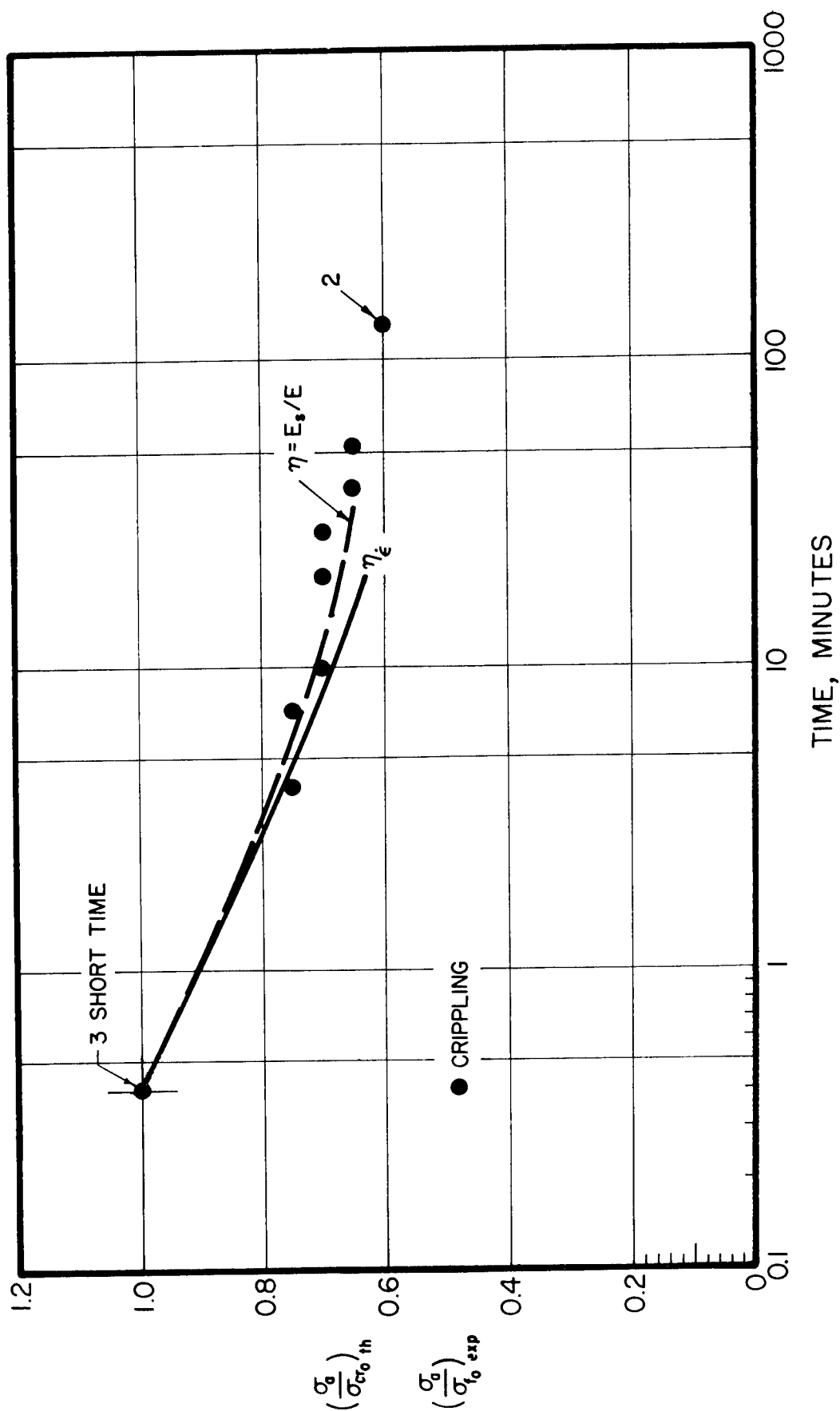


FIGURE 16 CORRELATION OF CREEP BUCKLING THEORY AND SECANT MODULUS APPROACH WITH EXPERIMENTAL CREEP CRIPPLING TIMES FOR LONG FLAT PLATES OF ALUMINUM ALLOY 2024-T3 AT 500°F UNDER AXIAL COMPRESSION WITH  $b/h = 23$  EXPRESSED IN NORMALIZED FORM.



## APPENDIX

The conventional method of simulating simple support boundary conditions involves the use of the vee groove-knife edge configuration. In an early series of experiments we adopted such a configuration and designed a specimen edge support jig containing vee grooves to receive plate specimens whose unloaded edges had been bevelled.

### A. Plate Jig Construction:

Vee grooves had been ground in Inconel-X segmented flat springs and these were mounted in a boxlike jig. Instrumentation was designed and constructed to measure end shortening and lateral deflection of the plate. End shortening measurements were made separately on the two unloaded plate edges by means of extensometers and the average end shortening was recorded. A parallelogram linkage, employed for lateral deflection, measured the maximum buckle amplitude on the plate irrespective of where it occurred. This instrumentation was similar in design to that shown in Figure 1.

It is necessary to measure both lateral deflection and end shortening and to obtain independently the pertinent compressive properties of the material. The lateral deflection measurements indicate when significant lateral deflections develop and when failure occurs. By comparing end shortening with the pertinent compressive data, the presence of unsuspected frictional effects which may be contributed by the supporting jig are detectable.

### B. Elastic Evaluation of Plate Jig:

Our past experience in conducting column buckling experiments indicated that short time tests in which the element undergoes elastic buckling are valuable to check out the supporting jig and the instrumentation. A comparison of the experimental buckling stress with the theoretical value indicates the efficacy of the support in simulating the theoretical boundary conditions. In a plate with initial imperfections it is difficult to ascertain when buckling has occurred since the element can continue to support load after buckling. However, Gerard (5) has shown that the failure or crippling of simply supported elastic plates can be determined from

$$\frac{\bar{\sigma}_f}{\sigma_{cy}} = 1.42 \left[ (h/b)(E/\sigma_{cy})^{1/2} \right]^{0.85} \quad (11)$$

The value of the numerical multiplier on the right hand side of Eq.(11) is determined by the boundary conditions on the unloaded edges and the 1.42 value is appropriate for simple support.

A series of tests were performed on long elastic plates of aluminum alloy 2024-T3 in the spring-vee groove supporting jig at room temperature. The approximate plate dimensions were 1 in. wide, 0.025 in. thick and 4.5 in. long with  $b/t = 40$ . Various values of edge clamping force were employed in

different experiments.

The test results for 4 specimens are shown in Figure 17 in the form of the end shortening vs. stress curves. For these specimens the value of the failure stress, as computed from Eq.(11) was found to be  $\bar{\sigma}_f = 27,300$  psi. The elastic buckling stress, computed from the conventional formula for simply supported plates was  $\sigma_{cr} = 25,000$  psi. These values are shown in Figure 17 together with the stress strain curve of the material as determined from compressive coupons tested in a compression jig.

In the first test, specimen EL-2, the edge supports were firmly clamped to the specimen introducing an appreciable in plane compressive stress perpendicular to the direction of loading. The failure stress for this specimen as shown in Figure 17 is within 0.4 percent of the theoretical value. However, the slope of the end shortening curve has a considerably higher value than that of the compressive stress strain curve.

In the second experiment with specimen EL-3, only enough edge force was introduced through the spring supports to assure the correct positioning of the specimen. The specimen failed at a stress of 23,200 psi as shown in Figure 17 which is lower than both the theoretical failure stress and the buckling stress. However, the end shortening response followed the compressive stress strain curve. The appearance of the failed specimen was typical of the buckling of a wide column on an elastic foundation.

The supporting jig was modified so that approximately 7 lbs. load could be applied through the edge supports to retain the specimen and prevent wide column buckling and failure. This introduced a stress of approximately 250 psi in the plane of the specimen perpendicular to the loading direction.

Two specimens were tested with the modified arrangement EL-4 and EL-5. As shown in Figure 17, the end shortening response follows the stress strain curve until approximately 23,000 psi. At this stress level, lateral deflections occur as indicated from the lateral deflection record (not shown) and the specimens fail within  $\pm 0.4$  percent of the theoretical value.

On the basis of the tests of EL-4 and EL-5 the simple support simulation jig was initially acceptable for the test program. It is interesting to note however that in the case where appreciable restraint was introduced, in specimen EL-2, the theoretical failure stress was still obtained, notwithstanding the fact that the specimen end shortening departs from the stress strain curve. This indicates that only at failure is the full applied load developed in the specimen and that prior to failure a portion of the applied load is taken out through friction by the supporting mechanism.

#### C. Initial Plate Tests at 500°F:

Plate specimens with  $b/h = 40$  and  $b/h = 25$  were machined from 0.040 in. thick aluminum alloy 2024-T3 and these were annealed to the 2024-0 condition

prior to testing. Compression test coupons were prepared in a similar manner and annealed together with the plate specimens. Short time compressive stress strain and creep tests were performed on the test coupons, the latter at a number of applied stress levels. Short time stress strain tests were performed on the coupons at an initial strain rate of  $.04 \text{ min}^{-1}$ , a value which was used for the short time plate tests and for the load application during the coupon creep and plate creep tests.

Short time and creep buckling tests were performed on plates using the same arrangement as had been employed in the elastic plate experiments. An allowance was made in the tightening procedure to take into account the differential expansion of specimen and jig in the heating to the  $500^{\circ}\text{F}$  test temperature.

When the end shortening data from plate tests were compared with the appropriate coupon data, it was found that for both the short time tests and the creep buckling tests the plate strain values were always well below those for the coupons at comparable stress levels and comparable times. Strain rate effects during loading were eliminated as a cause of the discrepancy.

On the other hand a calculation of the short time failure stress based upon Eq.(11) for  $b/h = 40$  plates indicated that the initial experimental data were within 5 percent of the theoretical values.

Frictional effects in the support mechanism were suspected as the cause of the discrepancy and an evaluation program was initiated to gain further insight into the experimentally revealed phenomena.

#### D. Evaluation Experiments on Plates at $500^{\circ}\text{F}$ :

1. Short Time Tests: End shortening data for the initial short time plate tests for  $b/h = 40$  are shown as curves 1, 2 and 3 in Figure 18. The average short time compressive stress strain curve is also shown. Theoretical values of the buckling stress and failure stress are also shown in the figure.

Two experiments were performed with a greatly reduced edge clamping force just sufficiently large to maintain specimen alignment. The end shortening response is shown as curves 4 and 5 in Figure 18. Here the experimental failure stress is below the theoretical value but above the buckling stress. The end shortening curve lies above the stress strain curve. The two specimens failed in the manner of wide columns on an elastic foundation.

In all five experiments there appeared to be frictional effects in the jig. It was suspected that during the heating process, minute creep distortions of the specimen edges in the small spaces between the vee groove spring segments were introducing longitudinal restraint on the specimen. The springs were replaced by solid blocks into which had been ground similar vee grooves to accommodate the plate specimen.

A second series of tests was performed using comparable edge clamping forces with the modified arrangement. The end shortening data for these experiments are shown in Figure 18. In curves 6 and 7 the edge clamping forces were comparable to those used in tests 1, 2 and 3. On the average there appears to be only a slight improvement in reducing friction. In the final short time experiment shown in curve 8 the clamping forces were comparable to those used in tests 4 and 5 and were just sufficiently large to position the specimen. The specimen failed below the theoretical buckling stress in the wide column mode. Yet even here friction has not been eliminated since the end shortening curve is still above the short time compressive stress-strain curve.

2. Creep Tests: A comparable series of evaluation experiments using the segmented spring and the solid vee groove edge supports was performed on  $b/h = 25$  plates at  $500^{\circ}\text{F}$  under an applied stress of 6,720 psi. For these plates the theoretical short time buckling stress  $\sigma_{cr} = 10,200$  psi, and the failure stress is in excess of 13,000 psi. The end shortening results are shown in Figure 19. Also shown in the figure are the lateral deflection data and the appropriate compressive creep data for the same applied stress level.

In the experiments for curves 9 and 10, spring vee groove supports were used with the normal clamping force. In the experiments for curves 11, 12 and 13 solid vee groove supports were employed.

If no frictional restraints were present we should expect the end shortening curve to follow the compressive creep curve until significant lateral deflections of the plate occurred. Thereafter, as the buckle wave form developed and lateral deflections increased, the end shortening curve should show larger creep strains in comparable times than the compressive creep curve. For all the data shown in Figure 7 the end shortening strains are lower than the creep strains even after significant lateral deflections have taken place and only just prior to failure does the end shortening increase above the creep curve. This is true for both types of supports although the solid support is somewhat superior to the segmented spring. In both however, the frictional effects are sufficiently large to preclude the use of the data for comparison with theory.

#### E. Conclusions:

Based upon the evaluation experiments, the following conclusions can be drawn:

1. The knife edge-vee groove arrangement can be employed to simulate simple support boundary conditions on elastic plates at room temperature.
2. At elevated temperatures in two different knife edge-vee groove configurations, there were significant frictional effects which served to restrain the end shortening of the plate.

3. Although frictional effects are present in knife edge-vee groove configurations, these effects appear to have little influence on the crippling strength of plates in short time experiments.

It was on the basis of this evaluation program that the vee groove-knife edge configuration was abandoned and the square tube configuration adopted.

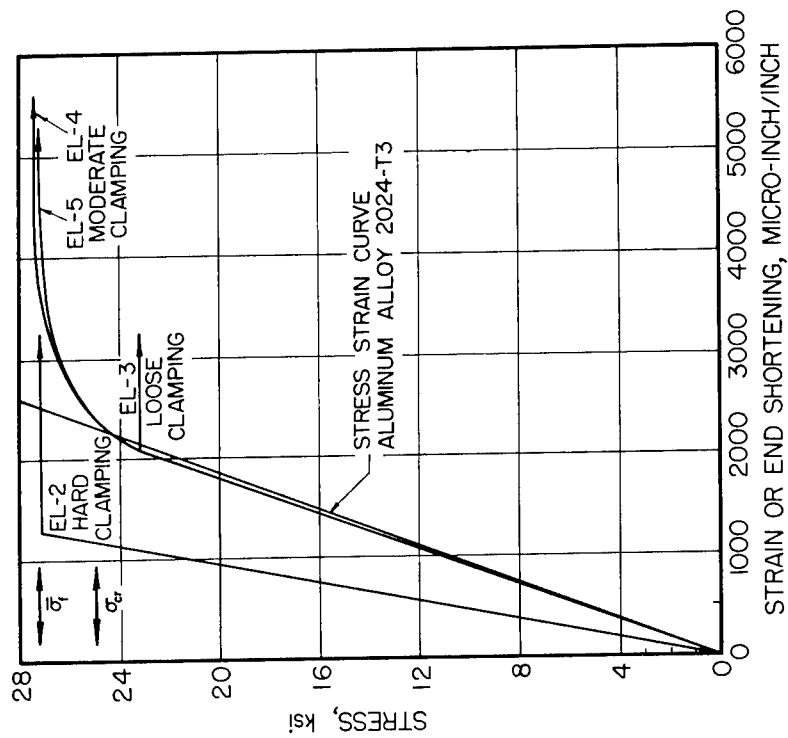


FIGURE 17 END SHORTENING DATA FOR ALUMINUM ALLOY 2024-T3 ELASTIC PLATES WITH  $b/h = 40$  AT ROOM TEMPERATURE. SIMPLE SUPPORT SIMULATED BY VEE GROOVE-KNIFE EDGE JIG.

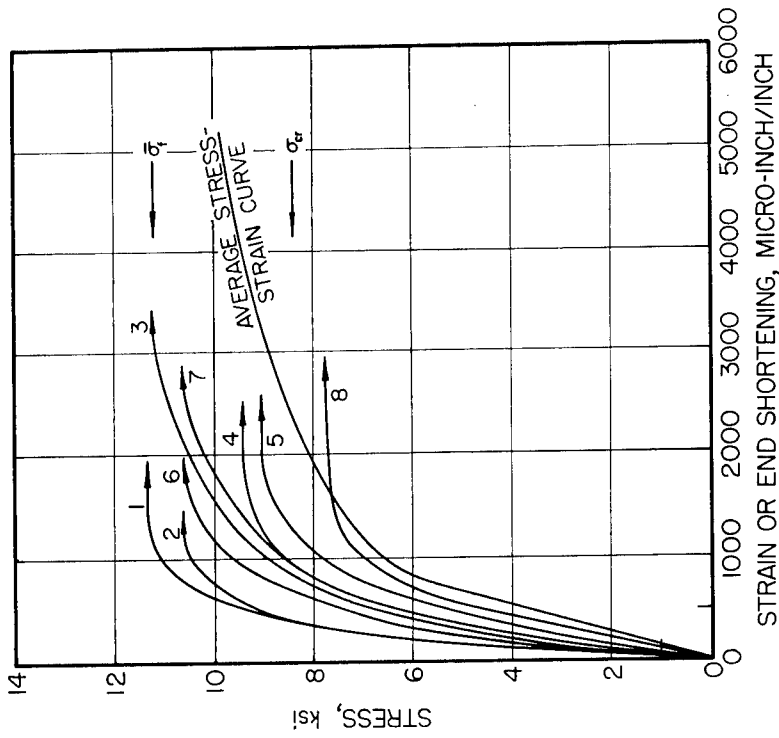


FIGURE 18 END SHORTENING DATA FOR ALUMINUM ALLOY 2024-O PLATES WITH  $b/h = 40$  AT 500°F SHOWN WITH COMPARABLE SHORT TIME COMPRESSIVE STRESS STRAIN DATA. SIMPLE SUPPORT SIMULATED BY VEE GROOVE-KNIFE EDGE JIG.

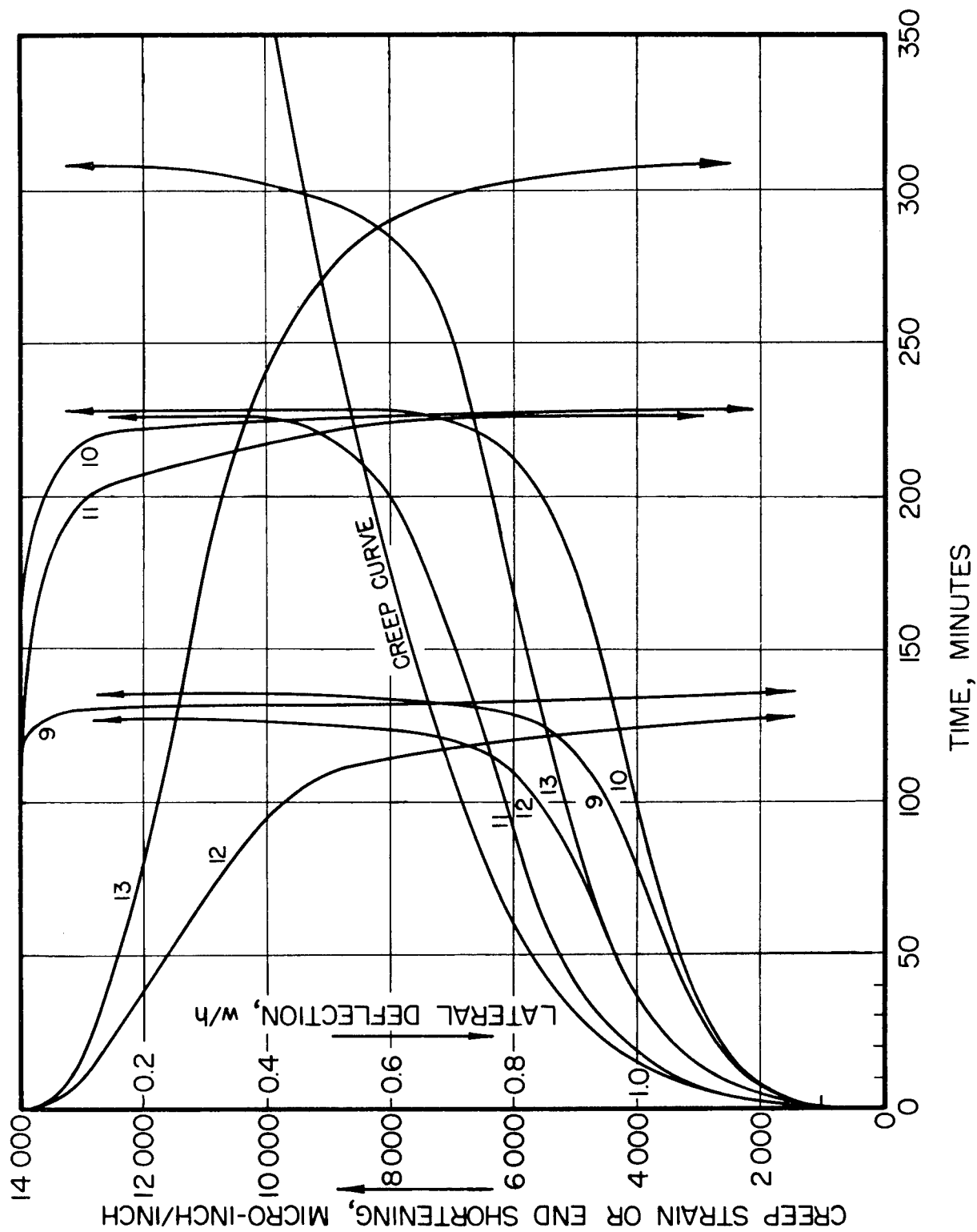


FIGURE 19 END SHORTENING AND LATERAL DEFLECTION DATA FOR CREEP BUCKLING EXPERIMENTS ON ALUMINUM ALLOY 2024-T3 PLATES WITH  $b/h = 25$  AT  $500^{\circ}\text{F}$  SHOWN WITH COMPARABLE COMPRESSIVE CREEP DATA AT AN APPLIED STRESS,  $\sigma_a = 6720$  psi. SIMPLE SUPPORT SIMULATED BY VEE GROOVE-KNIFE EDGE JIG.

1. Solid state physics
2. Deformation
- I. AFSC Project 7351 Task 735106
- II. Contract No. AF 33 (657)-8233
- III. New York University, New York, N. Y.
- IV. Ralph Papirno and George Gerard
- V. Avail. fr. OTS:
- VI. In ASTIA collection

Aeronautical Systems Division, Wright-Patterson Air Force Base, Ohio. Rpt. No. ASD-TDR-62-865. CORRELATION OF PLATE CREEP BUCKLING THEORY WITH EXPERIMENTS ON LONG PLATES OF ALUMINUM ALLOY 2024-0 AT 500°F. Final rpt. September 1962, 31 p. incl. figures.

Unclassified report  
The results of creep buckling experiments on long, simply supported plates of aluminum alloy 2024-0 at 500°F under axial compression were correlated with a previously developed theory for perfect plates. Compressive creep properties of the test material were obtained to develop the theoretical results. The plate experiments

( over )

were performed using a square tube configuration after an evaluation program indicated that the conventional vee groove-knife edge arrangement for simulating simple support was unsatisfactory for use at elevated temperatures. The theory was found to have predictive value for plate creep buckling when used in normalized form. A simplified approach for predicting creep crippling was also correlated with the test data.

1. Solid state physics
2. Deformation
- I. AFSC Project 7351 Task 735106
- II. Contract No. AF 33 (657)-8233
- III. New York University, New York, N. Y.
- IV. Ralph Papirno and George Gerard
- V. Avail. fr. OTS:
- VI. In ASTIA collection

Aeronautical Systems Division, Wright-Patterson Air Force Base, Ohio. Rpt. No. ASD-TDR-62-865. CORRELATION OF PLATE CREEP BUCKLING THEORY WITH EXPERIMENTS ON LONG PLATES OF ALUMINUM ALLOY 2024-0 AT 500°F. Final rpt. September 1962, 31 p. incl. figures.

Unclassified report  
The results of creep buckling experiments on long, simply supported plates of aluminum alloy 2024-0 at 500°F under axial compression were correlated with a previously developed theory for perfect plates. Compressive creep properties of the test material were obtained to develop the theoretical results. The plate experiments

( over )

were performed using a square tube configuration after an evaluation program indicated that the conventional vee groove-knife edge arrangement for simulating simple support was unsatisfactory for use at elevated temperatures. The theory was found to have predictive value for plate creep buckling when used in normalized form. A simplified approach for predicting creep crippling was also correlated with the test data.



Aeronautical Systems Division, Wright-Patterson Air Force Base, Ohio. Rpt. No. ASD-TDR-62-865. CORRELATION OF PLATE CREEP BUCKLING THEORY WITH EXPERIMENTS ON LONG PLATES OF ALUMINUM ALLOY 2024-0 AT 500°F. Final rpt. September 1962, 31 p. incl. figures.

Unclassified report  
The results of creep buckling experiments on long, simply supported plates of aluminum alloy 2024-0 at 500°F under axial compression were correlated with a previously developed theory for perfect plates. Compressive creep properties of the test material were obtained to develop the theoretical results. The plate experiments

( over )

were performed using a square tube configuration after an evaluation program indicated that the conventional vee groove-knife edge arrangement for simulating simple support was unsatisfactory for use at elevated temperatures. The theory was found to have predictive value for plate creep buckling when used in normalized form. A simplified approach for predicting creep crippling was also correlated with the test data.

1. Solid state physics
2. Deformation
- I. AFSC Project 7351 Task 735106
- II. Contract No. AF 33 (657)-8233
- III. New York University, New York, N. Y.

- IV. Ralph Papirno and George Gerard
- V. Avail. fr. OTS:
- VI. In ASTIA collection

Aeronautical Systems Division, Wright-Patterson Air Force Base, Ohio. Rpt. No. ASD-TDR-62-865. CORRELATION OF PLATE CREEP BUCKLING THEORY WITH EXPERIMENTS ON LONG PLATES OF ALUMINUM ALLOY 2024-0 AT 500°F. Final rpt. September 1962, 31 p. incl. figures.

Unclassified report  
The results of creep buckling experiments on long, simply supported plates of aluminum alloy 2024-0 at 500°F under axial compression were correlated with a previously developed theory for perfect plates. Compressive creep properties of the test material were obtained to develop the theoretical results. The plate experiments

( over )

were performed using a square tube configuration after an evaluation program indicated that the conventional vee groove-knife edge arrangement for simulating simple support was unsatisfactory for use at elevated temperatures. The theory was found to have predictive value for plate creep buckling when used in normalized form. A simplified approach for predicting creep crippling was also correlated with the test data.